Journal of
Synchrotron Radiation

ISSN 0909-0495

Received 4 February 2008
Accepted 16 May 2008

On-line optical and X-ray spectroscopies with crystallography: an integrated approach for determining metalloprotein structures in functionally well defined states

Mark J. Ellis,[a] Steven G. Buffey,[a] Michael A. Hough[b] and S. Samar Hasnain[b]*

[a]Molecular Biophysics Group, STFC Daresbury Laboratory, Warrington WA4 4AD, UK, and [b]School of Biological Sciences, University of Liverpool, Liverpool L69 7ZB, UK.
E-mail: s.s.hasnain@liv.ac.uk

X-ray-induced redox changes can lead to incorrect assignments of the functional states of metals in metalloprotein crystals. The need for on-line monitoring of the status of metal ions (and other chromophores) during protein crystallography experiments is of growing importance with the use of intense synchrotron X-ray beams. Significant efforts are therefore being made worldwide to combine different spectroscopies in parallel with X-ray crystallographic data collection. Here the implementation and utilization of optical and X-ray absorption spectroscopies on the modern macromolecular crystallography (MX) beamline 10, at the SRS, Daresbury Laboratory, is described. This beamline is equipped with a dedicated monolithic energy-dispersive X-ray fluorescence detector, allowing X-ray absorption spectroscopy (XAS) measurements to be made *in situ* on the same crystal used to record the diffraction data. In addition, an optical microspectrophotometer has been incorporated on the beamline, thus facilitating combined MX, XAS and optical spectroscopic measurements. By uniting these techniques it is also possible to monitor the status of optically active and optically silent metal centres present in a crystal at the same time. This unique capability has been applied to observe the results of crystallographic data collection on crystals of nitrite reductase from *Alcaligenes xylosoxidans*, which contains both type-1 and type-2 Cu centres. It is found that the type-1 Cu centre photoreduces quickly, resulting in the loss of the 595 nm peak in the optical spectrum, while the type-2 Cu centre remains in the oxidized state over a much longer time period, for which independent confirmation is provided by XAS data as this centre has an optical spectrum which is barely detectable using microspectrophotometry. This example clearly demonstrates the importance of using two on-line methods, spectroscopy and XAS, for identifying well defined redox states of metalloproteins during crystallographic data collection.

Keywords: combined X-ray methods; XAS; optical spectroscopy; crystallography; microspectrophotometer; radiation damage; metalloproteins.

1. Introduction

The foremost part of our knowledge of protein structure and function is based on X-ray crystallography using synchrotron radiation. Metalloproteins comprise more than 30% of the proteins in a genome, and many of these use the redox properties of metals to catalyse enzymatic reactions. A particular issue in the study of metalloproteins by X-ray crystallography is whether the crystal structure is a true representation of the protein in a functionally relevant metal redox state.

In this context, X-ray-induced photoreduction of metal centres in proteins is a phenomenon which is of increasing concern to experimentalists using the highly intense X-ray beams produced by third-generation synchrotron radiation sources. The majority of the incident X-ray energy absorbed by a protein crystal is *via* the photoelectric effect (Burmeister, 2000; Murray *et al.*, 2005). The photoexcited electrons produced in this way can readily reduce redox centres in metalloproteins and measures have to be taken that either minimize or monitor these X-ray-induced effects.

As an example, consider the case of photosystem II, where X-ray absorption spectroscopy (XAS) data showed that the expected Mn(IV) cluster had become 80% photoreduced to biologically inactive Mn(II) by X-rays at less than the absorbed dose used for determining the crystal structure (Yano *et al.*, 2005). Similarly, rapid photoreduction of three different haem proteins with varying redox potential has been shown using single-crystal optical spectroscopy (Beitlich *et al.*, 2007). Importantly, in many cases it is non-trivial to identify changes in metal oxidation states using structural changes visible by X-ray crystallography alone, even at high resolution. We note that such photon-induced changes in oxidation state (and hence in X-ray absorption edge position) may also cause problems during multiwavelength anomalous diffraction (MAD) phasing experiments.

Where the protein contains a chromophore, spectroscopic measurements can be made on individual crystals (Hadfield & Hajdu, 1993; Mozzarelli & Rossi, 1996) and, as a response to these issues, increasing attention has been given to combining X-ray diffraction with single-crystal spectroscopies (Royant *et al.*, 2007; Carpentier *et al.*, 2007). For optically active metalloproteins, single-crystal microspectrophotometry may be used to monitor the metal centres and a key advance has been the incorporation of microspectrophotometers onto X-ray beamlines (on-line single-crystal spectroscopy) (Chen *et al.*, 1994; Hadfield & Hajdu, 1993; Sakai *et al.*, 2002). Through this approach, diffraction and optical spectroscopic data may be collected on the same crystal without the need to remove the sample from the beamline. To this end, macromolecular crystallography (MX) beamlines at a number of synchrotron sources, including the Swiss Light Source and ESRF, have been equipped with microspectrophotometers. These instruments have been used to monitor the redox state of intermediates generated during X-ray exposure of a methylamine dehydrogenase–amicyanin complex, thus allowing tailored data-collection protocols to be developed such that the structures of each intermediate could be determined (Pearson *et al.*, 2007). In some cases, X-ray-driven reduction of metal centres may allow intermediate states in an enzymatic mechanism to be accessed (Schlichting *et al.*, 2000).

Although optical microspectrophotometry is a powerful technique, it suffers from a major limitation in that many metal centres are optically silent in biologically relevant oxidation states (Table 1*a*). These include the important Cu(I) and Zn(II) states which are optically [and EPR (electron paramagnetic resonance)] silent owing to their d^{10} nature. Other metal sites, such as type-2 Cu centres, may contain an optically active metal but the resulting spectrum may be too weak and difficult to measure in a crystal, as is the case for copper nitrite reductase, an enzyme under study in this paper. Also, in proteins that contain several different optically active metal centres, it may not be possible to monitor the site with the weaker absorbance. An example would be sulfite oxidase where the optical spectrum of the molybdenum cofactor is entirely masked by that of the haem centre (Kisker, 2001).

XAS, in contrast, is generally applicable to metal centres in any oxidation state (Table 1*b*). The complementarity of protein crystallography (PX) with solution XAS studies was noted (Hasnain & Hodgson, 1999; Hasnain & Strange, 2003) and capabilities to combine these methods on the same crystal were implemented on the MX beamline 10 at the SRS (Cianci *et al.*, 2005; Arcovito *et al.*, 2007) and at SSRL (Latimer *et al.*, 2005; Yano *et al.*, 2006). SRS beamline 10 is fully tunable over a wavelength range of 0.873 Å to 2.3 Å (5.45–14.21 keV) with a normal operating range of 0.92 Å to 2.07 Å (5.99–13.47 keV) delivering a flux of $\sim 10^{11}$ photons s^{-1}. This energy range covers X-ray absorption edges for many of the biologically important 3*d* transition metals (Table 1*b*). Recently, we have exploited this beamline to combine X-ray diffraction and polarized XANES measurements on crystals of cyanomyoglobin (Arcovito *et al.*, 2007).

The end-station of the beamline is composed of a MAR desktop beamline (DTB) with cryogenic sample changer, with a MARMosaic 225 CCD detector for recording diffraction data and an Ortec C-TRAIN-04 detector for measuring XAS data (Derbyshire *et al.*, 1999). Here we describe an extension to these capabilities through the incorporation of a single-crystal microspectrophotometer into the goniometry, thus allowing optical spectra to be collected *in situ* and in parallel with X-ray diffraction and high-quality XAS data. The combination of two spectroscopies allows the status of both optically active and optically silent metal centres to be monitored during a crystallographic experiment (see Hough *et al.*, 2008).

2. Description of the experimental apparatus

A microspectrophotometer based on the 4DX Uppsala system (Hadfield & Hajdu, 1993; Wilmot *et al.*, 2002) has been installed on SRS MAD beamline 10. Two light sources, halogen or halogen/deuterium, may be used to provide good spectral intensities in the UV–visible region (350–800 nm). A 50 µm fibre-optic cable transmits the light to a collimating lens/reflecting objective. The focal point of the light emitted by the objective is centred on the crystal some 24 mm away with a typical spot size of $\sim$25 µm. A second collimating lens/reflecting objective at the same distance from the sample passes the transmitted light *via* a 400 µm fibre-optic cable and through a 50 µm slit to an Oriel MS125 spectrograph equipped with a 400 lines mm^{-1} diffraction grating. The dispersed spectrum is then measured using an Andor DV401A-UV CCD detector (1024 × 127 pixels) operating at 213 K.

To incorporate the microspectrophotometer into the DTB, an easily attachable/removable mounting arc was designed that extends over the χ axis. In this configuration, one objective is behind and above the crystal and the second is below and in front of the crystal (Fig. 1). The arc is designed to be easily removable from the DTB to allow for a rapid transition between operation of the beamline with and without the instrument. Two guide pins and two screws locate and fix the arc into the DTB. A modified alignment tool has been designed specifically for the beamline, and the microspectrophotometer can be fitted and aligned ready for use in approximately 30 min. The positioning of the instrument is

Table 1
(*a*) Optical properties of selected metalloproteins and (*b*) X-ray absorption energies and main oxidation states of 3*d* metals found in proteins.

(*a*) The major peak in the optical spectrum between 350 and 800 nm is given. Note that Zn(II) and Cu(I) are always optically silent. The optical spectra of Mo centres are generally masked by the Fe centres occurring in the same proteins. 'Weak' optical spectra are difficult to measure using a single-crystal microspectrophotometer.

Metal	Example protein	Redox state	Optical properties	Main peak (nm) / ε (M^{-1} cm^{-1})	Reference
Cobalt	Methionine synthase	Co(III)	Strong	352 / 20200	Banerjee & Matthews (1990)
		Co(II)	Strong	475 / 9470	
		Co(I)	Strong	525 / 10000	
Copper	Azurin (type-1 Cu)	Cu(II)	Strong	620 / 5700	Colczak *et al.* (2001)
		Cu(I)	Silent	–	
	Cu, Zn superoxide dismutase (type-2 Cu)	Cu(II)	Weak	680 / 300	McCord & Fridovich (1969)
		Cu(I)	Silent	–	
	Galactose oxidase (type-2 Cu)	Cu(II)	Strong	445 / 6500	McPherson *et al.* (2001)
	Catechol oxidase (type-3 Cu)	Cu(II)	Weak	580 / 450	Eicken *et al.* (2001)
Iron: haem	Haemoglobin	Fe(III) oxy	Strong	541 / 13500	Di Iorio (1981)
		Fe(III) deoxy	Strong	555 / 12500	
	Cytochrome c	Fe(III)	Strong	410 / 100000	Banci & Assfalg (2001)
		Fe(II)	Strong	413 / 125000	
Iron: Fe–S proteins	Rubredoxin	Fe(III)	Strong	490 / 6600	Meyer & Moulis (2001)
		Fe(II)	Silent	–	
Manganese	Mn superoxide dismutase	Mn(III)	Weak	478 / 850	Stroupe *et al.* (2001)
		Mn(II)	Silent	–	
	Arginase	Mn(II)	Silent	–	Bewley & Flanagan (2001)
Nickel	Ni superoxide dismutase	Ni(III)	Strong	378 / 6000	Bryngelson & Maroney (2007)
		Ni(II)	Weak	450 / $<$500	
Vanadium	Vanadium haloperoxidase	V(V)	Silent	–	Wever & Hemrika (2001)

(*b*) The energy of an absorption edge will vary with changes of the metal oxidation state and the nature of the ligand environment. For example, for vanadium complexes the edge shift can vary by up to $\pm$5 eV per unit oxidation and by up to $\pm$2.5 eV for changes of ligation for the same oxidation state (Frank *et al.*, 1998). X-ray absorption energies are taken from Thompson *et al.* (2001).

	K-edge absorption energy		
Metal	(Å)	(eV)	Oxidation states
Cobalt	1.608	7709.0	+2, +3
Copper	1.381	8979.0	+1, +2
Iron	1.743	7112.0	+2, +3, +4
Manganese	1.896	6540.0	+2, +3, +4
Nickel	1.488	8333.0	+2
Vanadium	2.269	5465.0	+2, +3, +4, +5
Zinc	1.284	9659.0	+2

such that it does not interfere with the operation of the nitrogen cryostream and so data using all three techniques (optical spectroscopy, XAS, MX) may be collected at either room temperature or temperatures down to 100 K. This configuration allows the optical light path to be centred using the crystal microscope such that it intersects the same volume of the crystal as the X-ray beam, and allows both diffraction and XAS data to be measured without removing the crystal from the system. This in turn allows both the optical spectroscopic and XAS monitoring of the oxidation states of metal centres during crystallographic data collection.

Alignment of the objectives to the centred-sample position is conducted using an in-house alignment tool mounted on a Hampton pin adapter. This allows manual fine alignment of the light spot from the source to the cross hairs of the crystal-alignment camera. The Andor CCD detector may be calibrated to wavelength using a Holmium filter built into the light source. A series of test data were measured to ensure that the addition of the new instrument into the beamline goniometry did not significantly interfere with the normal measurement of crystallographic or XAS data. The correct operation of the fluorescence detector with the microspectrophotometer was confirmed by collection of data from metal foils, while test X-ray diffraction data were collected to a resolution limit of $\sim$1.5 Å.

3. Experimental methods and results

3.1. Copper nitrite reductase from *Alcaligenes xylosoxidans*

In order to test the capabilities of this currently unique experimental facility, we have undertaken a combined optical–XAS-crystallographic study of crystals of copper nitrite reductase from *Alcaligenes xylosoxidans* (*Ax*NiR). *Ax*NiR

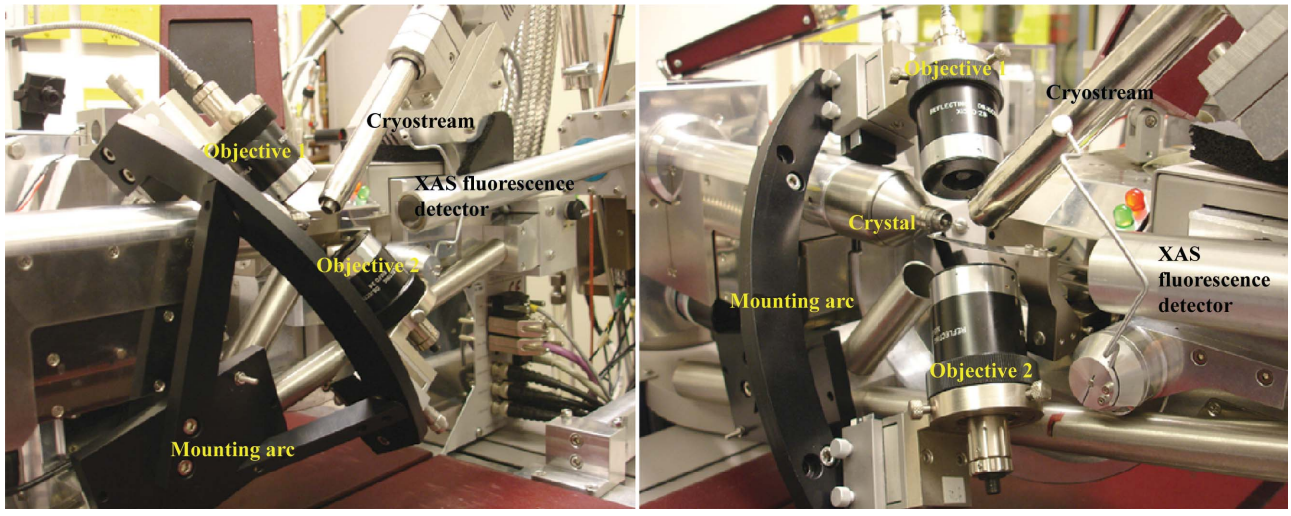

Figure 1
Views of the microspectrophotometer as installed on SRS beamline 10. A mounting arc allows for easy fitting of the instrument onto the MAR DTB. The cryostream and C-TRAIN fluorescence detector are unaffected by the addition of the mounting arc, thus allowing optical spectroscopic, XAS and crystallographic data to be collected from the same crystal.

contains both an optically active type-1 Cu (T1Cu) centre and a type-2 Cu (T2Cu) centre that has weak absorbance (Abraham *et al.*, 1993)[1] and is thus essentially optically silent with the current detection capabilities of the microspectrophotometer. The two copper centres are linked *via* a Cys–His bridge where T1Cu ligates to Cys and T2Cu ligates to His. Both Cu centres are in the Cu(II) oxidation state in the resting enzyme. Under physiological conditions the T1Cu receives an electron from a partner protein, azurin. It has been shown that electron transfer from T1Cu to T2Cu is gated and is triggered by the conformational changes resulting from the binding of nitrite to T2Cu, replacing the water molecule ligated to T2Cu in the resting state (Strange *et al.*, 1999; Hough *et al.*, 2005).

X-ray irradiation can be used to introduce electrons into the protein crystal that may be selectively taken up by metal centres, resulting in their reduction. By combining the three techniques described above, both metal centres may be monitored and the effect of X-ray exposure on redox state can be characterized. Recombinant native *Ax*NiR was produced as described previously (Prudencio *et al.*, 1999). Crystals in space group *R*3 were grown by the hanging-drop vapour-diffusion method. A drop containing 2 µl of 10 mg ml^{-1} protein solution was mixed with an equal volume of reservoir solution containing 20% PEG550 MME, 10 m*M* $ZnSO_4$ and 100 m*M* MES pH 6.0. Crystals grew in one week and were intense blue in colour.

3.2. Optical, XAS and MX data collection from *Ax*NiR crystals

Crystals were transferred into a cryoprotectant solution consisting of mother liquor with a PEG550 MME concentration of 35% before mounting in a nitrogen cryostream at 100 K. Optical spectra were either an accumulation of 20 exposures each of 0.05 s duration or were single 0.5 s exposures measured at regular time intervals. Data were analysed using the Andor iDus software package. Background and reference spectra were measured with the crystal translated out of the light path. A crystal orientation was chosen such that the crystal spectrum matched the solution spectrum of *Ax*NiR.

A crystal of *Ax*NiR was exposed to a continuous flux of X-rays of wavelength 1.37 Å. The effect of this X-ray radiation exposure on the optical spectrum is shown in Fig. 2(*a*).[2] The size (in absorbance units) of the 595 nm peak as a function of absorbed X-ray dose is given in Fig. 2(*b*). X-ray doses were calculated using the program *RADDOSE* (Murray *et al.*, 2005) and included the absorption contributions from sulfur and metal atoms. In brief, photon fluxes were calculated from photodiode measurements carried out at the sample position. These photodiode measurements were referenced against the ionization chamber readings inside the collimator system of the MAR DTB allowing calculation of the flux incident on the sample position. Crystal sizes were measured using a graticule on one of the objectives on the microscope. These optical spectroscopic data indicate that the T1Cu centre was rapidly photoreduced from the Cu(II) to Cu(I) oxidation state by X-ray exposure. We note that the X-ray dose sufficient to predominantly reduce the T1Cu centres is modest in comparison with doses commonly used in the determination of high-resolution crystal structures.

Cu *K*-edge X-ray absorption data were collected in fluorescence mode using an energy-resolving four-element monolithic germanium C-TRAIN-4 detector (Ortec) (Derbyshire *et al.*, 1999). A silicon (111) double-crystal monochromator with

[1] The T1Cu centre exhibits an intense optical absorption spectrum. The T2Cu centre shows only a very weak absorption, which is non-detectable from these crystals.

[2] Optical spectra were single 0.5 s exposures.

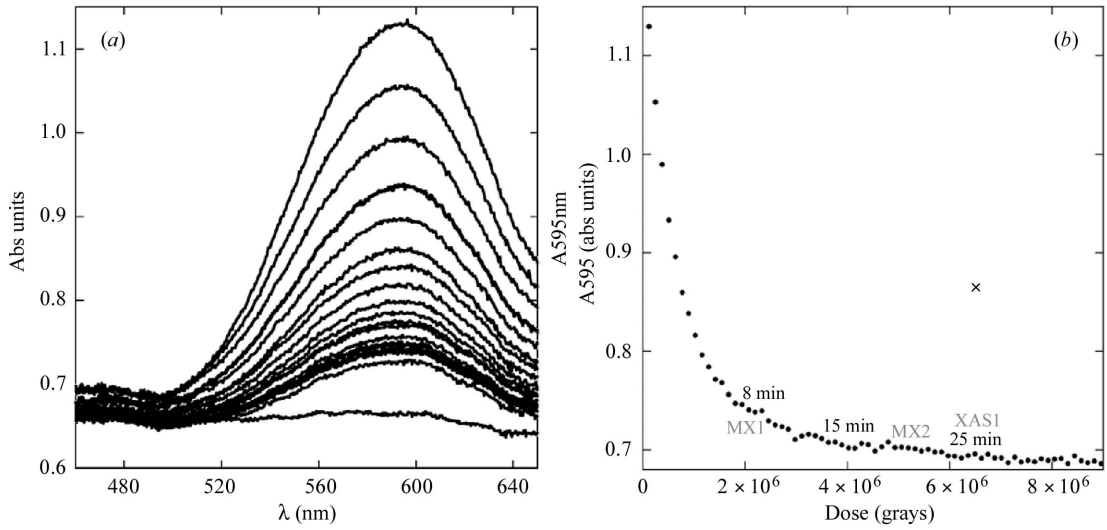

Figure 2
Dose-dependent X-ray-induced photoreduction of a static *Ax*NiR crystal using 1.37 Å X-rays. (*a*) Spectra collected at 30 s intervals showing the progressive reduction in the height of the 595 nm peak associated with conversion of T1Cu(II) to T1Cu(I). The first 20 spectra and the final spectrum are plotted. (*b*) The dependence of the 595 nm peak height on absorbed X-ray dose. The time points indicative of MX and XAS data collection are shown.

an energy resolution of $\sim 1 \times 10^{-4}$ eV was used (Cianci *et al.*, 2005). XAS spectra consisted of 168 data points over the energy range 8.96–9.11 keV with a dwell time of 1 s per point. Data were processed using the Daresbury Laboratory programs *EXCALIB* and *EXBACK*. X-ray diffraction data were measured using a MAR 225 CCD and processed using *HKL2000* (Otwinowski & Minor, 1997), the structures solved by molecular replacement in *PHASER* (McCoy *et al.*, 2007) and refined in *REFMAC5* (Murshudov *et al.*, 1997).

Each of the three crystallographic data sets (MX1, MX2 and MX3) consisted of 100 X-ray exposures each of 10 s. Following the collection of the second X-ray data set, a Cu *K*-edge XAS spectrum was measured. An optical spectrum[3] was collected from the crystal following each X-ray and the XAS data set. We note that all optical and XAS measurements were taken at the same crystal position and orientation in order to eliminate any changes in the spectrum that might arise from a change in orientation. In all cases, data using these three techniques were collected on the same crystal on-line at 100 K. Data collection parameters are given in Table 2.

The type-2 Cu centre is essentially optically silent, and so to monitor its status we have combined the information obtained from the Cu *K*-edge XAS data with the crystal structures. The XAS spectra following the determination of the second and third crystal structures are given in Fig. 3. Note that the 8984 eV edge feature, characteristic of the Cu(I) redox state in the T2Cu centre (Fig. 3 inset), is not observed, consistent with the T2Cu site remaining in the Cu(II) oxidized state although the optical data (not shown) indicate that the T1Cu centre is essentially completely reduced to Cu(I) at this point. The Cu–OH_2 distance in the three crystal structures is similar to that expected for an oxidized T2Cu centre (Fig. 4, Table 3), suggesting that the photoreduction of the T2Cu centre is much less rapid than that of the T1Cu centre and that structure MX3 is of the T1Cu(I)–T2Cu(II) form, *i.e.* where the two Cu centres are in different redox states.

Table 2
Data collection, refinement and model statistics.

Values in parentheses are for the outer resolution shell (1.95–1.90 Å).

	MX1	MX2	MX3
Data collection			
Wavelength (Å)	0.98	0.98	0.98
Space group	*R*3	*R*3	*R*3
Cell dimensions: *a*, *b*, *c* (Å)	89.1, 89.1, 288.3	89.1, 89.1, 288.3	89.1, 89.1, 288.4
Resolution (Å)	1.90	1.90	1.90
R_{merge}	3.9 (12.4)	3.8 (13.6)	4.1 (16.1)
$I/\sigma(I)$	20.3 (3.8)	20.3 (4.8)	20.6 (4.0)
Completeness (%)	97.7 (81.2)	97.8 (82.2)	97.7 (81.1)
Wilson *B*-factor (Å^2)	19.5	19.6	20.9
No. unique reflections	66937	65482	65507
Refinement			
R_{work}	0.162	0.162	0.162
R_{free}	0.201	0.197	0.195
ESU (Å)	0.12	0.12	0.12
No. protein atoms	5228	5198	5206
No. water molecules	696	642	670
Average *B*-factor			
Protein (Å^2)	18.6	18.5	19.9
Water (Å^2)	31.0	30.1	32.7
RMS deviations			
Bond lengths (Å)	0.011	0.011	0.011
Bond angles (°)	1.30	1.32	1.32
Ramachandran plot			
Most favoured (%)	90.1	89.5	90.6
PDB accession code	2vw7	2vw4	2vw6

4. Conclusions

A single-crystal microspectrophotometer has been successfully integrated into the fully tunable MAD beamline 10 at the

[3] Accumulation of 20 × 0.05 s exposures.

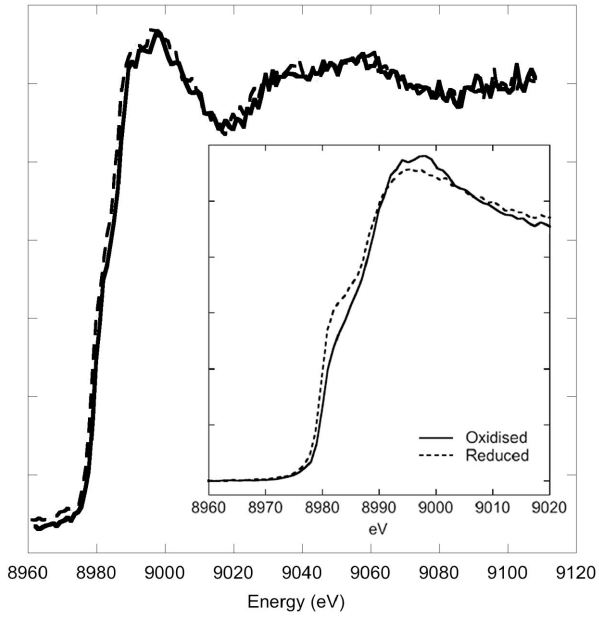

Figure 3
XAS spectra from the *Ax*NiR crystal following the collection of structures MX2 (solid line) and MX3 (dotted line) using 0.98 Å X-rays. The spectra are consistent with a T2Cu(II) oxidation state in both cases. Inset: comparison of the edge region for oxidized and fully reduced *Ax*NiR crystals. Note that the oxidized crystal has been exposed only to the X-rays used to collect the XAS spectrum. In the reduced spectrum the 8984 eV shoulder arising from T2Cu(I) is apparent.

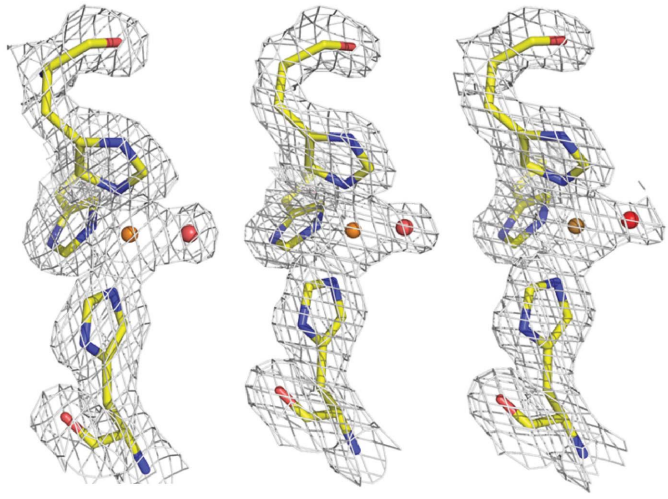

Figure 4
Electron density maps contoured at 1σ from crystal structures (*a*) MX1, (*b*) MX2 and (*c*) MX3. The copper atom is shown as an orange sphere. Note that a water molecule is coordinated to the T2Cu centre in all cases, along with three histidine ligands. The four-coordinate geometry and clear density for the Cu-coordinated water molecule (shown as a red sphere) clearly indicate that this centre is in the oxidized Cu(II) form, consistent with the XAS data.

SRS, resulting in the unique capability of measuring the on-line optical spectrum together with high-quality XAS and X-ray diffraction data from a crystal *in situ*. This development allows the monitoring of the status of metal centres in metalloproteins during a crystallographic experiment. The capability for such monitoring is becoming increasingly important with the higher X-ray doses which can be delivered by beamlines on third-generation synchrotron radiation sources. We have used crystals of the copper nitrite reductase from *A. xylosoxidans* as a test case. Optical spectroscopy revealed that the T1Cu centre was rapidly reduced by exposure to X-rays. To determine the oxidation state of the optically silent T2Cu centre, XAS measurements were performed on the same crystal, showing that the edge features indicative of reduced T2Cu centres were not present. Combined with the diffraction data, these observations showed that the crystal structures collected were in the mixed T1[red]–T2[ox] form, consistent with previous biochemical, kinetic and structural observations on *Ax*NiR in the solution state, that electron transfer from T1Cu to T2Cu is gated (Strange *et al.*, 1999; Hough *et al.*, 2005). The combination of these three techniques applied to a single crystal allows monitoring of both optically active and optically silent metal centres during a crystallographic experiment. This approach provides a model for the design of MX/PX beamlines on current and future generations of synchrotron radiation sources.

Table 3
Cu–ligand parameters for the crystallographic data sets.

Numbers in parentheses refer to the second *Ax*NiR monomer in the crystallographic asymmetric unit.

	Cu–water distance (Å)	Cu *B*-factor (Å^2)	Water *B*-factor (Å^2)
MX1	1.93 (1.90)	18 (17)	18 (19)
MX2	1.86 (1.93)	16 (18)	17 (18)
MX3	1.89 (1.91)	18 (19)	20 (19)

We thank Mr Neil Bliss, Mr Steve Postlethwaite and Mr David Robinson (Engineering and Instrumentation Department, STFC Daresbury Laboratory) for designing the microspectrophotometer mounting arc for the station. We thank STFC for provision of beam time and funds. Beamline 10 is supported by BBSRC grant number BBE001971 and the work on nitrite reductase by BBSRC grant number BBD0162901 to SSH.

References

Abraham, Z. H. L., Lowe, D. J. & Smith, B. E. (1993). *Biochem. J.* **295**, 587–595.
Arcovito, A., Benfatto, M., Cianci, M., Hasnain, S. S., Nienhaus, K., Nienhaus, G. U., Savino, C., Strange, R. W., Vallone, B. & Della Longa, S. (2007). *Proc. Natl. Acad. Sci. USA*, **104**, 6211–6216.
Banci, L. & Assfalg, M. (2001). *Handbook of Metalloproteins*, edited by A. Messerschmidt, R. Huber, T. Poulos and K. Wieghardt, pp. 33–43. Chichester: John Wiley and Sons.
Bannerjee, R. V. & Matthews, R. G. (1990). *FASEB J.* **4**, 1450–1459.
Beitlich, T., Kühnel, K., Schulze-Briese, C., Shoeman, R. L. & Schlichting, I. (2007). *J. Synchrotron Rad.* **14**, 11–23.
Bewley, M. C. & Flanagan, J. M. (2001). *Handbook of Metalloproteins*, edited by A. Messerschmidt, R. Huber, T. Poulos and K. Wieghardt, pp. 952–962. Chichester: John Wiley and Sons.
Bryngelson, P. A. & Maroney, M. J. (2007). *Met. Ions Life. Sci.* **2**, 417–444.
Burmeister, W. P. (2000). *Acta Cryst.* D**56**, 328–341.

Carpentier, P., Royant, A., Ohana, J. & Bourgeois, D. (2007). *J. Appl. Cryst.* **40**, 1113–1122.
Chen, L., Durley, R. C. E., Mathews, F. S. & Davidson, V. L. (1994). *Science*, **264**, 88–90.
Cianci, M. *et al.* (2005). *J. Synchrotron Rad.* **12**, 455–466.
Colczak, U., Dennison, C., Messerschmidt, A. & Canters, G. W. (2001). *Handbook of Metalloproteins*, edited by A. Messerschmidt, R. Huber, T. Poulos and K. Wieghardt, pp. 1170–1194. Chichester: John Wiley and Sons.
Derbyshire, G., Cheung, K.-C., Sangsingkeow, P. & Hasnain, S. S. (1999). *J. Synchrotron Rad.* **6**, 62–63.
Di Iorio, E. I. (1981). *Methods Enzymol.* **76**, 57–71.
Eicken, C., Gerdemann, C. & Krebs, B. (2001). *Handbook of Metalloproteins*, edited by A. Messerschmidt, R. Huber, T. Poulos and K. Wieghardt, pp. 1319–1329. Chichester: John Wiley and Sons.
Frank, P., Hodgson, K. O., Kustin, K. & Robinson, W. O. (1998). *J. Biol. Chem.* **273**, 24498–24503.
Hadfield, A. & Hajdu, J. (1993). *J. Appl. Cryst.* **26**, 839–842.
Hasnain, S. S. & Hodgson, K. O. (1999). *J. Synchrotron Rad.* **6**, 852–864.
Hasnain, S. S. & Strange, R. W. (2003). *J. Synchrotron Rad.* **10**, 9–15.
Hough, M. A., Antonyuk, S. V., Strange, R. W., Eady, R. R. & Hasnain, S. S. (2008). *J. Mol. Biol.* **378**, 353–361.
Hough, M. A., Ellis, M. J., Antonyuk, S., Strange, R. W., Sawers, G., Eady, R. R. & Hasnain, S. S. (2005). *J. Mol. Biol.* **350**, 300–309.
Kisker, C. (2001). *Handbook of Metalloproteins*, edited by A. Messerschmidt, R. Huber, T. Poulos and K. Wieghardt, pp. 1121–1135. Chichester: John Wiley and Sons.
Latimer, M. J., Ito, K., McPhillips, S. E. & Hedman, B. (2005). *J. Synchrotron Rad.* **12**, 23–27.
McCord, J. M. & Fridovich, I. (1969). *J. Biol. Chem.* **244**, 6049–6055.
McCoy, A. J., Grosse-Kunstleve, R. W., Adams, P. D., Winn, M. D., Storoni, L. C. & Read, R. J. (2007). *J. Appl. Cryst.* **40**, 658–674.
McPherson, M. J., Parsons, M. R., Spooner, R. K. & Wilmot, C. W. (2001). *Handbook of Metalloproteins*, edited by A. Messerschmidt, R. Huber, T. Poulos and K. Wieghardt, pp. 1272–1283. Chichester: John Wiley and Sons.
Meyer, J. & Moulis, J. M. (2001). *Handbook of Metalloproteins*, edited by A. Messerschmidt, R. Huber, T. Poulos and K. Wieghardt, pp. 505–517. Chichester: John Wiley and Sons.
Mozzarelli, A. & Rossi, G. L. (1996). *Annu. Rev. Biophys. Biomol. Struct.* **25**, 343–365.
Murray, J. W., Rudiño-Piñera, E., Owen, R. L., Grininger, M., Ravelli, R. B. G. & Garman, E. F. (2005). *J. Synchrotron Rad.* **12**, 268–275.
Murshudov, G. N., Vagin, A. A. & Dodson, E. J. (1997). *Acta Cryst.* D**53**, 240–255.
Otwinowski, Z. & Minor, W. (1997). *Methods Enzymol.* **276**, 307–326.
Pearson, A. R., Pahl, R., Kovaleva, E. G., Davidson, V. L. & Wilmot, C. M. (2007). *J. Synchrotron Rad.* **14**, 92–98.
Prudencio, M., Eady, R. R. & Sawers, G. (1999). *J. Bacteriol.* **181**, 2323–2329.
Royant, A., Carpentier, P., Ohana, J., McGeehan, J., Paetzold, B., Noirclerc-Savoye, M., Vernède, X., Adam, V. & Bourgeois, D. (2007). *J. Appl. Cryst.* **40**, 1105–1112.
Sakai, K., Matsui, Y., Kouyama, T., Shiro, Y. & Adachi, S. (2002). *J. Appl. Cryst.* **35**, 270–273.
Schlichting, I., Berendzen, J., Chu, K., Stock, A. M., Maves, S. A., Benson, D. E., Sweet, R. M., Ringe, D., Petsko, G. A. & Sligar, S. G. (2000). *Science*, **287**, 1615–1622.
Strange, R. W., Murphy, L. M., Dodd, F. E., Abraham, Z. H. L., Eady, R. R., Smith, B. E. & Hasnain, S. S. (1999). *J. Mol. Biol.* **287**, 1001–1009.
Stroupe, M. E., DiDonato, M. & Tainer, J. A. (2001). *Handbook of Metalloproteins*, edited by A. Messerschmidt, R. Huber, T. Poulos and K. Wieghardt, pp. 941–951. Chichester: John Wiley and Sons.
Thompson, A. *et al.* (2001). *X-ray Data Handbook*, edited by D. Vaughan. Lawrence Berkeley National Laboratory, Berkeley, CA, USA.
Wever, R. & Hemrika, W. (2001). *Handbook of Metalloproteins*, edited by A. Messerschmidt, R. Huber, T. Poulos and K. Wieghardt, pp. 1417–1428. Chichester: John Wiley and Sons.
Wilmot, C. M., Sjogren, T., Carlsson, G. H., Berglund, G. I. & Hajdu, J. (2002). *Methods Enzymol.* **353**, 301–318.
Yano, J., Kern, J., Irrgang, K. D., Latimer, M. J. Bergmann, U., Glatzel, P., Pushkar, Y., Biesiadka, J., Loll, B., Sauer, K., Messinger, J., Zouni, A. & Yachandra, V. K. (2005). *Proc. Natl. Acad. Sci. USA*, **102**, 12047–12052.
Yano, J., Kern, J., Sauer, K., Latimer, M. J., Pushkar, Y., Biesiadka, J., Loll, B., Saenger, W., Messinger, J., Zouni, A. & Yachandra, V. K. (2006). *Science*, **314**, 821–825.